

Analysis of Temperature and Magnetic Field Distribution in Superconducting Bulk During Pulsed Field Magnetization

Hiroyuki Fujishiro, Tomoyuki Naito, and Daiki Furuta

Abstract—We have constructed the framework of theoretical simulation for magnetic field and temperature in the superconducting bulk during pulsed field magnetization (PFM) using finite element method (FEM). Three successive pulsed field applications with identical strength (SPA) were performed to the cryo-cooled bulk and time and spatial dependence of local field $B_z(t, (z, r))$ and temperature $T(t, (z, r))$ were calculated. The trapped field B_z increased and the maximum temperature rise T_{max} decreased with increasing pulse number. The B_z enhancement results from the decrease in temperature rise because of the already trapped flux. The results of the simulation well reproduced the experimental ones qualitatively.

Index Terms—Pulsed field magnetization, simulation, superconducting bulk.

I. INTRODUCTION

PULSED field magnetization (PFM) for REBaCuO bulks (RE: rare earth element or Y) has been intensively investigated for practical applications as a substitute for field-cooled magnetization (FCM). The trapped field B_z by PFM is, however, lower than that by FCM because of the large temperature rise by the dynamical motion of the magnetic flux. To enhance B_z , it has been believed that the reduction in temperature rise ΔT and the lowering of starting temperature T_s are effective because of the enhancement of the critical current density J_c , similarly for FCM. A multi-pulse application such as an iteratively magnetizing pulsed-field method with reducing amplitude (IMRA) [1] and a multi-pulse technique with step-wise cooling (MPSC) [2] is effective to enhance B_z . We have proposed a new PFM technique named a modified MPSC (MMPSC) and successfully realized the highest field trap of $B_z = 5.20$ T on the $\phi 45$ mm GdBaCuO bulk at 30 K [3], which is a record-high value by PFM to date. To understand the PFM phenomena in detail and to enhance the B_z value, it is necessary to use the aid of a theoretical simulation because the experimental research has been limited.

Several theoretical studies for PFM have been reported [4], [5]. We have also constructed the framework of theoretical simulation in the superconducting bulk with homogeneous superconducting properties after a single magnetic pulse application and reproduced the experimental results [6]. As described in this

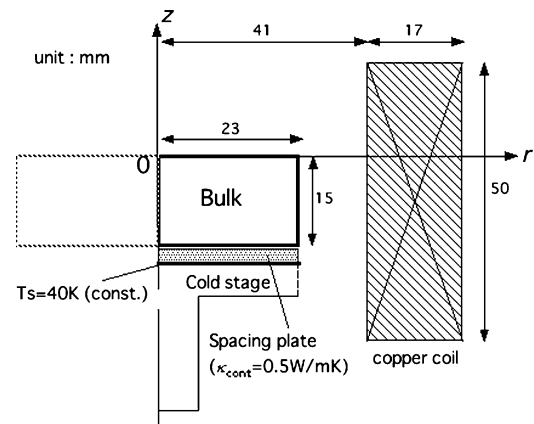


Fig. 1. Model and dimensions around the bulk and solenoid copper coil for pulsed field magnetization (PFM).

paper, we applied the theoretical simulation to the successive pulsed field application with identical strength (SPA) for the superconducting bulk, and time and spatial dependence of local field $B_z(t, r)$ and temperature $T(t, r)$ were calculated.

II. MODELING AND THEORETICAL SIMULATION

Based on our experimental setup around the bulk, the framework of the theoretical simulation was constructed. As shown in Fig. 1, a superconducting bulk disk 46 mm in diameter and 15 mm in thickness was stacked on the cold stage of the refrigerator in a vacuum chamber and cooled to the starting temperature $T_s = 40$ K. In the simulation, the bulk was magnetized using a solenoid-type copper coil. Physical phenomena during PFM are described by electromagnetic and thermal equations on the axisymmetric coordinate in the following, which were referred from ref. [7] using a commercial software PHOTO-EDDY-THERMO (PHOTON Ltd., Japan).

$$\frac{\partial}{\partial r} \left[\frac{\nu}{r} \frac{\partial}{\partial r} (r \mathbf{A}) \right] + \frac{\partial}{\partial z} \left(\nu \frac{\partial \mathbf{A}}{\partial z} \right) = J_0 + J \quad (1)$$

$$\rho C \frac{\partial T}{\partial t} = \frac{1}{r} \frac{\partial}{\partial r} \left(r \kappa_{ab} \frac{\partial T}{\partial r} \right) + \frac{\partial}{\partial z} \left(\kappa_c \frac{\partial T}{\partial z} \right) + Q, \quad (2)$$

where \mathbf{A} is the magnetic vector potential, ν the magnetic reluctivity, ρ the mass density, J_0 the coil current density, J the superconducting current density or induced current density, and Q is the heat generation. In (2), C ($= 1.32 \times 10^2$ J/kgK) is the specific heat, κ_{ab} ($= 20$ W/mK) and κ_c ($= 4$ W/mK) are the thermal conductivity of the bulk in the ab -plane and along the c -axis, respectively [8].

Manuscript received August 01, 2010; accepted October 13, 2010. Date of publication November 29, 2010; date of current version May 27, 2011.

The authors are with the Faculty of Engineering, Iwate University, Morioka 020-8551, Japan (e-mail: fujishiro@iwate-u.ac.jp).

Digital Object Identifier 10.1109/TASC.2010.2089419

The J value is given by the following equation:

$$J = \sigma E = -\sigma \frac{\partial \mathbf{A}}{\partial t}, \quad (3)$$

where E is the electric field and σ the electric conductivity. The FEM analysis of the coupled problem with electromagnetic field and heat diffusion was performed.

The power- n model ($n = 8$) was used to describe the non-linear $E - J$ characteristic in superconducting bulk [7].

$$E = E_c \left(\frac{J}{J_c} \right)^n, \quad (4)$$

where J_c is the critical current density and E_c (1×10^{-6} V/m) is the reference electric field. The magnetic field dependence of the J_c was described by the Kim model:

$$J_c = J_{c0} \frac{B_0}{|B| + B_0}, \quad (5)$$

where J_{c0} is J_c for $B = 0$ and B_0 ($= 1.3$ T) is constant [7]. The temperature dependence of J_{c0} is described by the following equation,

$$J_{c0} = \alpha \left\{ 1 - \left(\frac{T}{T_c} \right)^2 \right\}^{\frac{3}{2}}, \quad (6)$$

where T_c is the critical temperature ($= 92$ K) and α is the strength of J_{c0} . $\alpha = 4.6 \times 10^8$ A/m² was used in the analysis which represents $J_{c0} = 3.3 \times 10^8$ A/m² at 40 K. Iterative calculation was performed to obtain the convergence of σ in the superconductor at each time step. The applied pulsed field $B_{ex}(t)$ with the rise time of $\tau = 0.01$ s was approximated in the following equation;

$$B_{ex}(t) = B_{ex} \frac{t}{\tau} \exp\left(1 - \frac{t}{\tau}\right). \quad (7)$$

Three magnetic pulses from No. 1 to No. 3 with the identical strength of $B_{ex} = 4$ to 8 T were sequentially applied.

III. EXPERIMENTAL RESULTS

We magnetized the SmBaCuO bulk by the SPA method at 40 K experimentally [9]. Fig. 2(a) and (b) present the pulse number dependence of the trapped field B_z and the maximum temperature rise ΔT_{max} at the center of the bulk surface. The time interval between each pulse was 20 min., for which the bulk was re-cooled to T_s . The largest amount of the flux was trapped during the No. 1 pulse to the virgin state bulk and B_z was gradually enhanced with increasing pulse number. In Fig. 2(b), ΔT_{max} monotonically decreases and approaches a steady value with increasing pulse number for each B_{ex} . Fig. 2(c) shows the time dependence of the local field $B_z(t)$ and the temperature $T(t)$ at the center of the bulk surface for the SPA method of $B_{ex} = 4.64$ T. The applied pulsed field $B_{ex}(t)$ is also shown. $B_z(t)$ for the No. 1 pulse becomes maximum at $t = 0.02$ s and then decreases with increasing time and approaches to the final value of $B_z = 2.8$ T. $T(t)$ for the No. 1 pulse takes a maximum at $t = 15$ s and then decreases concomitantly with increasing time. T_{max} decreases with increasing pulse number.

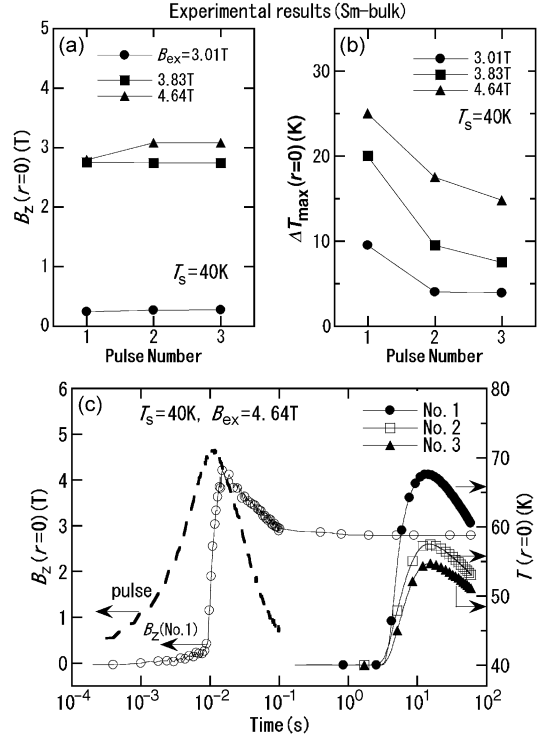


Fig. 2. Experimental results of pulse number dependence of the (a) trapped field B_z and (b) maximum temperature rise ΔT_{max} at the center of the Sm-BaCuO bulk. (c) Time dependence of the local field $B_z(t)$ and the temperature $T(t)$ at $r = 0$ for the SPA method of $B_{ex} = 4.64$ T.

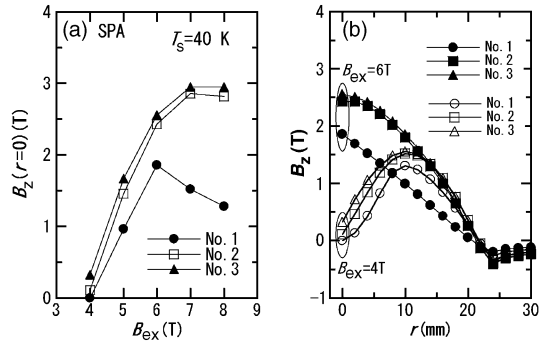


Fig. 3. (a) Results of simulation for the pulse number dependence of the trapped field $B_z(r = 0)$ at the center of the bulk surface as a function of applied field B_{ex} . (b) Cross sections of the trapped field $B_z(r)$ profiles of the SPA for $B_{ex} = 4$ and 6 T.

It is noteworthy that the time, at which $B_z(t)$ takes a maximum, is about three orders of magnitude faster than the time, at which $T(t)$ takes a maximum. $B_z(t)$ and $T(t)$ described in Fig. 2 are common features for the PFM procedure.

IV. RESULTS OF SIMULATION AND DISCUSSION

Fig. 3(a) depicts the results of the simulation for the pulse number dependence of the trapped field $B_z(r = 0)$ at the center of the bulk surface as a function of applied field B_{ex} . For the No. 1 pulse, $B_z(r = 0)$ starts to increase for $B_{ex} = 4$ T, becomes maximum for 6 T and then decreases with further increase in B_{ex} . The $B_z(r = 0)$ increases for the No. 2 pulse and tends

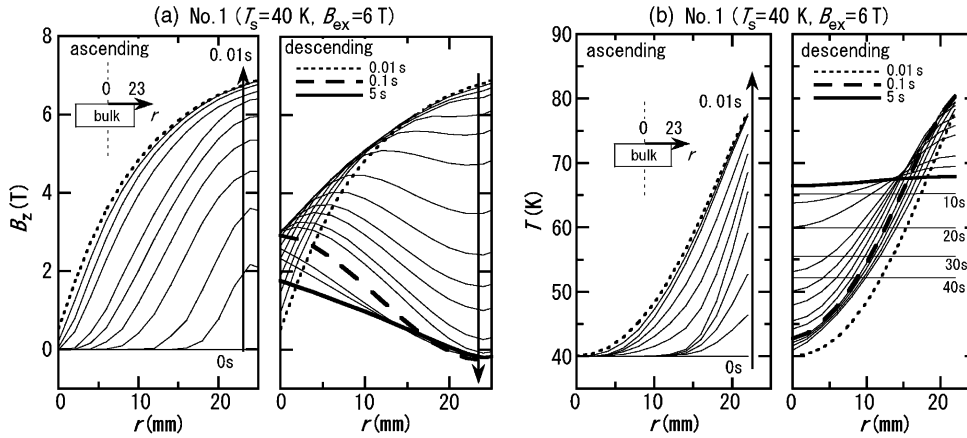


Fig. 4. Time evolution and spatial distribution of the (a) local magnetic field $B_z(t, r)$ and (b) temperature $T(t, r)$ on the bulk surface after applying No. 1 pulsed field of $B_{ex} = 6$ T.

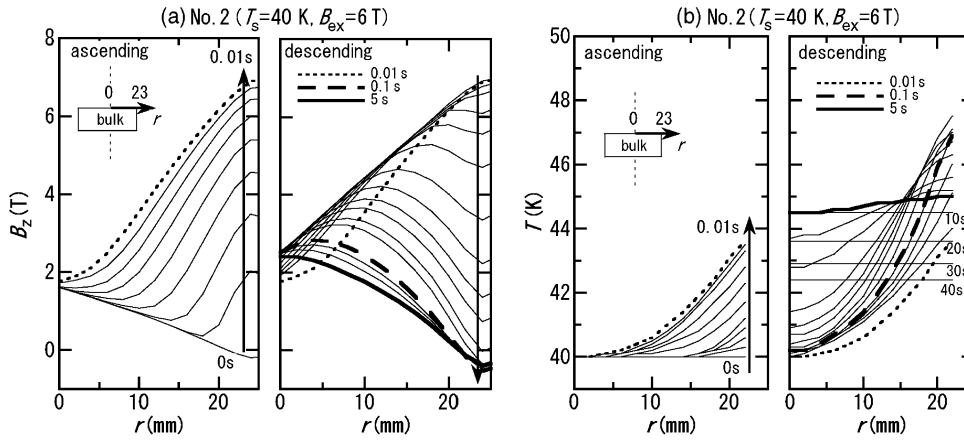


Fig. 5. Time evolution and spatial distribution of the (a) local magnetic field $B_z(t, r)$ and (b) temperature $T(t, r)$ on the bulk surface after applying No. 2 pulsed field of $B_{ex} = 6$ T.

to saturate for the No. 3 pulse for each B_{ex} . Fig. 3(b) shows the cross section of the trapped field profile $B_z(r)$ of the SPA for $B_{ex} = 4$ and 6 T. The positions of $r = 0$ and 23 mm are the center and edge on the bulk surface, respectively. For $B_{ex} = 4$ T, the $B_z(r)$ profile was concave and the trapped field slightly increased with increasing pulse number. On the other hand, for $B_{ex} = 6$ T, the $B_z(r)$ profile was convex for the No.1 pulse and $B_z(r = 0)$ value increased fairly for the No. 2 pulse.

Fig. 4(a) and (b), respectively, present the time evolution and spatial distribution of the local magnetic field $B_z(t, r)$ and the temperature $T(t, r)$ on the bulk surface after applying a No. 1 pulsed field of $B_{ex} = 6$ T. The left and right parts for each figure are for the ascending ($t \leq 0.01$ s) and descending ($t \geq 0.01$ s) stages, respectively. For the ascending stage, the magnetic flux intrudes gradually into the bulk from the bulk periphery and magnetic gradient increases with approach to the bulk center at $t = 0.01$ s. For the descending stage, the magnetic field decreased gradually at the outer region with increasing time. On the other hand, local field near the bulk center increased to 3 T at $t = 0.1$ s and then decreased gradually to $B_z = 1.7$ T at the steady state. In Fig. 4(b), the temperature $T(t)$ at the bulk periphery gradually increased with time at the ascending stage,

e.g., $T = 78$ K at $t = 0.01$ s. However, the temperature for $r = 0$ remained as 40 K. At the descending stage, the generated heat diffuses to the bulk center gradually. After an isothermal temperature profile took place along the r -direction at $t = 5$ s, the temperature decreased with increasing time. In this case, temperature gradient existed along the z -direction because the bottom of the bulk was fixed at 40 K.

Fig. 5(a) and (b) depict $B_z(t, r)$ and $T(t, r)$ on the bulk surface after applying No. 2 pulsed field of $B_{ex} = 6$ T. For the ascending stage, the magnetic flux intrudes gradually into the bulk from the bulk periphery. For the descending stage, the magnetic field decreased gradually at the outer region with increasing time. The local field near the bulk center increased to 2.7 T at $t = 0.1$ s and then decreased gradually to $B_z = 2.3$ T at $t = 5$ s. In Fig. 5(b), the $T(t, r)$ behavior is similar time and radius dependences to that for the No. 1 pulse, but the temperature rise is fairly reduced; $T_{max} = 44.5$ K at $t = 7$ s.

Let us summarize the results of the simulation. Fig. 6(a) and (b) show the pulse number dependence of the trapped field B_z and the maximum temperature rise ΔT_{max} on the bulk center. $B_z(r = 0)$ increased concomitantly with increasing pulse number and then saturated and increased with increasing B_{ex} . The ΔT_{max} value for $r = 0$ monotonically

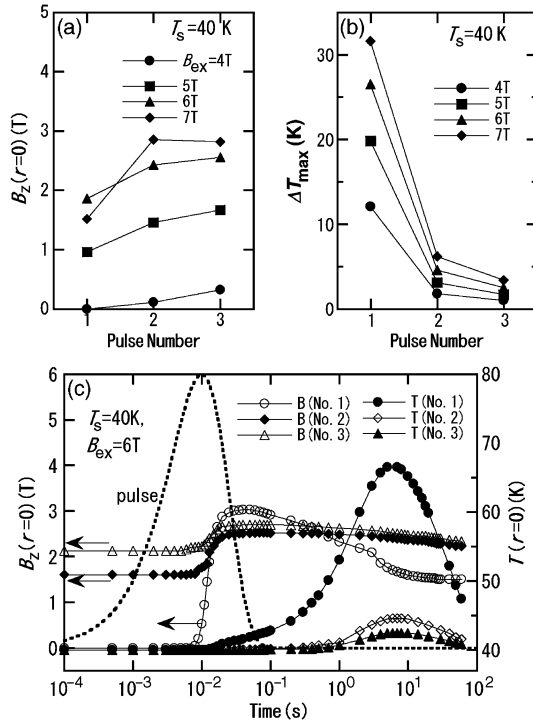


Fig. 6. Results of the simulation for the pulse number dependence of the (a) trapped field B_z and (b) maximum temperature rise ΔT_{max} on the bulk center for various B_{ex} values at 40 K. (c) Time dependence of the local field $B_z(t)$ and the temperature $T(t)$ at the center of the bulk surface for the SPA method of $B_{ex} = 6$ T.

decreases and approaches a steady value with increasing pulse number. These results reproduced the experimental results presented in Fig. 2(a) and (b) qualitatively. Fig. 6(c) shows the time dependence of the local field $B_z(t)$ and the temperature $T(t)$ at the center of the bulk surface for the SPA method of $B_{ex} = 6$ T. The applied pulsed field $B_{ex}(t)$ with a rise time of $\tau = 0.01$ s is also described. $B_z(t)$ for the No. 1 pulse takes a maximum at $t = 0.02$ s and then decreases with increasing time and approaches to the final value of $B_z = 1.5$ T. On the other hand, the peak value of $B_z(t)$ decreases but the final value of B_z increases slightly. The simulated $T(t)$ for the No. 1 pulse takes a maximum of 67 K at $t = 7$ s and then decreases with increasing time. The time, at which $T(t)$ takes a maximum, is decided by the thermal conductivity of the bulk

crystal (κ_{ab}, κ_c) and the cooling power and is independent of the pulse number. T_{max} decreases with increasing pulse number. The time delay between the $B_z(t)$ peak and the $T(t)$ peak is of about three orders of magnitude, which is nearly the consistent of the experimental results as presented in Fig. 2(c).

V. CONCLUSION

We have constructed the framework of theoretical simulation for magnetic field and temperature in the superconducting bulk during pulsed field magnetization (PFM). Three successive pulsed field with identical strength (No. 1 - No. 3) were applied to the cryo-cooled bulk and time and spatial dependence of local field $B_z(t, r)$ and temperature $T(t, r)$ were calculated. The trapped field B_z increased and the maximum temperature rise T_{max} decreased with increasing pulse number. The B_z enhancement comes from the decrease in temperature rise because of the already trapped flux. The results of the simulation well reproduced the experimental results qualitatively.

REFERENCES

- [1] Y. Yanagi, Y. Itoh, M. Yoshikawa, T. Oka, T. Hosokawa, H. Ishihara, H. Ikuta, and U. Mizutani, "Trapped field distribution on Sm-Ba-Cu-O bulk superconductor by pulsed-field magnetization," in *Advances in Superconductivity XII*. Tokyo: Springer-Verlag, 2000, pp. 470–474.
- [2] M. Sander, U. Sutter, R. Koch, and M. Klatser, "Pulsed magnetization of HTS bulk parts at $T < 77$ K," *Supercond. Sci. Technol.*, vol. 13, pp. 841–845, 2000.
- [3] H. Fujishiro, T. Tateiwa, A. Fujiwara, T. Oka, and H. Hayashi, "Higher trapped field 5 T on HTSC bulk by modified pulse field magnetizing," *Physica C*, vol. 445–448, pp. 334–338, 2006.
- [4] K. Berger, J. Leveque, D. Netter, B. Douine, and A. Rezzoug, "Influence of Temperature and/or Field Dependences of the $E - J$ Power Law on Trapped Magnetic Field in Bulk YBaCuO," *IEEE Trans. Appl. Supercond.*, vol. 17, pp. 3028–3031, 2007.
- [5] R. Shiraishi and H. Ohsaki, "Flux Dynamics in Inhomogeneous Bulk Superconductor During Pulsed Field Magnetization," *IEEE Trans. Appl. Supercond.*, vol. 16, pp. 1794–1797, 2006.
- [6] H. Fujishiro and T. Naito, "Simulation of temperature and magnetic field distribution in superconducting bulk during pulsed field magnetization," *Supercond. Sci. Technol.*, vol. 23, no. 10, 2010.
- [7] Y. Komi, M. Sekino, and H. Ohsaki, "Three-dimensional numerical analysis of magnetic and thermal fields during pulsed field magnetization of bulk superconductors with inhomogeneous superconducting properties," *Physica C*, vol. 469, pp. 1262–1265, 2009.
- [8] H. Fujishiro and S. Kohayashi, "Thermal conductivity, thermal diffusivity and thermoelectric power of Sm-bBased Bulk Superconductors," *IEEE Trans. Appl. Supercond.*, vol. 12, pp. 1124–1127, 2002.
- [9] H. Fujishiro, K. Yokoyama, T. Oka, and K. Noto, "Temperature rise in an Sm-based bulk superconductor after applying iterative pulse fields," *Supercond. Sci. Technol.*, vol. 17, pp. 51–57, 2004.